

Stratigraphic filtering and source penetration depth

Mirko van der Baan^{1*}, James Wookey^{2†} and Dirk Smit³

¹*School of Earth and Environment, Earth Sciences, University of Leeds, Leeds, LS2 9JT, UK,* ²*Department of Earth Sciences, University of Bristol, Bristol, BS8 1RJ, UK, and* ³*Shell International Exploration and Production, Volmerlaan 8, Postbus 60, 2280 AB Rijswijk, The Netherlands*

Received January 2006 revision accepted January 2007

ABSTRACT

Seismic exploration underneath highly heterogeneous layers such as basalt flows is possible by lowering the principal source frequency. Unfortunately this also reduces resolution. Wave-localization theory is a multiple scattering theory that can be used to study stratigraphic filtering in chaotic lithologies. It predicts the apparent attenuation due to scattering of a plane wave traversing a layer with high velocity fluctuations. It can therefore predict the optimum principle source frequency in the trade-off between loss of resolution and increased penetration depth. We show how this can be done with the help of a few statistical parameters derived from a well-log analysis; namely, the average background velocity, the expected standard deviation in the velocity fluctuations, the typical scale length of the heterogeneities and the thickness of the basalt layer. In the likely situation that no local well logs exist, a multitude of scenarios can easily be examined at low cost.

INTRODUCTION

Seismic exploration in highly heterogeneous media is beset with challenges. Multiple scattering in a layer with large velocity variations may prevent penetration of seismic energy, thereby effectively shielding any potential exploration targets that lie underneath. Examples include the Atlantic Margin in north-west Europe, where there are areas with abundant basaltic flows that blanket underlying sedimentary layers, and potential reservoirs underneath coral reefs or sequences of coal layers. All are often opaque to seismic illumination.

Ziolkowski *et al.* (2003) proposed using low-frequency sources to render highly heterogeneous layers effectively homogeneous. Multiple scattering is greatly reduced if the principal source frequency is lowered, thus increasing the amount of coherent energy that penetrates the obstructing layers.

Figures 1 and 2 illustrate the concept on a synthetic model. A 600 m thick basalt layer overlies two deeper reflections.

The basalt layer is based on a true well log through a basalt. Two synthetic sections are created for a source positioned at the surface (Fig. 1). In the first case, we use a 50 Hz Ricker wavelet, while a 10 Hz wavelet is used for the second simulation. Figure 2 shows the resulting sections. Hardly any coherent energy is visible underneath the top-basalt reflection for the high-frequency wavelet, whereas the low-frequency section reveals the sub-basalt structures.

However, the use of low-frequency sources also reduces the bandwidth and thereby the resolution. Therefore, a trade-off exists between an increased source-penetration depth and a reduction in resolution. The question thus becomes: Can we predict the frequency content of sub-basalt reflections for a given geology and source spectrum? In other words, can we determine the optimum source frequency before acquisition? We need a frequency-dependent multiple scattering theory to answer these questions.

First, we introduce such a multiple-scattering theory, and then we illustrate how it can be used to predict the recorded spectrum of reflected plane waves for a variety of randomly layered media. Finally, we outline the proposed work-flow to compute the source penetration depth while taking stratigraphic filtering into account.

* E-mail: mvdbaan@earth.leeds.ac.uk

† Formerly School of Earth and Environment, Earth Sciences, University of Leeds, Leeds LS2 9JT, UK

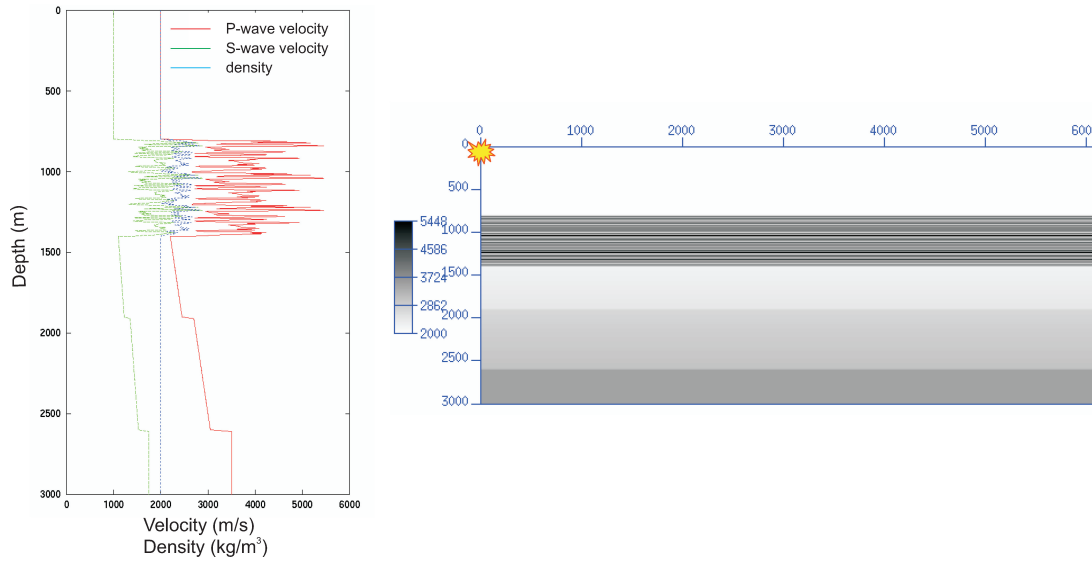


Figure 1 Synthetic 1D model used for numerical simulations. A 600 m thick basalt layer taken from a well log exists together with two deeper reflections (deep 1 and deep 2). Left: P- and S-wave velocities and density profiles. Right: P-wave velocity model and source position.

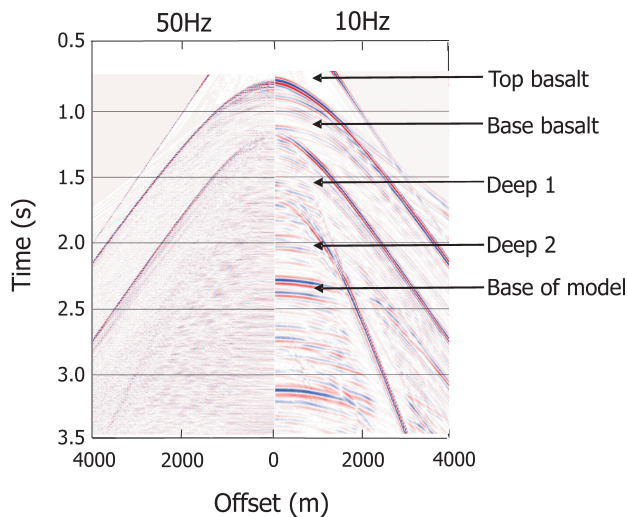


Figure 2 Resulting synthetic gathers for a 50 Hz (left) and a 10 Hz (right) Ricker wavelet. Lowering the source frequency reduces scattering inside the basalt layer and renders any sub-basalt structures visible but also lowers resolution. Can we predict the optimum source frequency before acquisition?

WAVE-LOCALIZATION THEORY AND STRATIGRAPHIC FILTERING

Wave-localization theory is a multiple scattering theory that stems from the quantum theory of disordered solids (Anderson 1958). It proves that the amplitude of a plane wave traversing a chaotic 1D medium decays exponentially with propagation depth due to apparent scattering losses (van der Baan 2001;

van der Baan 2002), i.e. the transmission coefficient T of the plane wave behaves as follows:

$$\lim_{L \rightarrow \infty} |T| = \exp[-\gamma_{sc} L], \quad (1)$$

where γ_{sc} is the Lyapunov coefficient and L is the thickness of the medium. The Lyapunov coefficient γ_{sc} describes the apparent attenuation due to scattering.

A matched medium is considered to determine the apparent attenuation of the plane wave. The random layer is sandwiched between two homogeneous half-spaces with matching density ρ_0 and P-wave velocity c_0 . The background density ρ_0 and velocity c_0 are assumed to be constant, and relative fluctuations δc occur in the velocity only. The medium is described therefore by

$$c(z) = \begin{cases} c_0, & z < 0, z > L, \\ c_0[1 + \delta c(z)], & 0 \leq z \leq L, \end{cases} \text{ and } \rho(z) = \rho_0 \text{ everywhere.} \quad (2)$$

For simplicity, we only treat the acoustic problem to prevent P-S and S-P conversions. This is not a problem since we will only consider vertical incidence where no P-S conversions occur. The fluctuations are also assumed to be stationary.

The stationarity assumption is important. It allows us to employ a statistical description of the medium instead of a deterministic one. Each velocity variation with depth has to be known in the latter case, whereas a statistical description only requires knowledge of the type of autocorrelation

function ϕ_c describing the velocity fluctuations, its magnitude and characteristic scale length. This reduces the number of degrees of freedom significantly, thereby facilitating our analysis for source penetration depth.

It is not unusual for relative velocity fluctuations $\delta c(z)$ to be described by an exponential autocorrelation function (White, Sheng and Nair 1990). This function is given by

$$\phi_c(\zeta) = \sigma_c^2 \exp[-|\zeta/a|], \quad (3)$$

where σ_c denotes the standard deviation of the relative velocity fluctuations δc , a denotes the typical scale length of the heterogeneities, and ζ denotes the depth lag.

Shapiro and Zien (1993) considered a plane wave impinging from above on the inhomogeneous medium, and applied a second-order perturbation on the resulting wave equation to determine the appropriate Lyapunov coefficient γ_{sc} . In this way, they showed that, for vertical incidence,

$$\gamma_{sc} = \frac{1}{4} k_0^2 \int_0^\infty \phi_c(\zeta) \cos(2k_0\zeta) d\zeta, \quad (4)$$

where $k_0 = 2\pi f/c_0$ is the vertical wavenumber in the background medium for frequency f .

Substitution of the exponential autocorrelation function (3) into the general expression for the Lyapunov coefficient (4) leads to the desired Lyapunov coefficient γ_{exp} for exponential media. It is given by (Shapiro and Zien 1993; van der Baan 2001)

$$\gamma_{exp} = \frac{4\sigma_c^2 \pi^2 f^2 a}{16\pi^2 f^2 a^2 + c_0^2}. \quad (5)$$

Substitution of the Lyapunov coefficient (5) for exponential media into expression (1) produces an equation that describes the amplitude of a plane wave traversing a chaotic medium as a function of frequency f , the thickness L of the basalt layer, and some basic properties related to the geology, such as the standard deviation σ_c of the velocity fluctuations and their characteristic scale length a . Figure 3 shows, for instance, the frequency-dependent amplitude behaviour for the synthetic model shown in Fig. 1. The amplitude of the 50 Hz wavelet is clearly attenuated considerably faster than that of the 10 Hz wavelet for increasing layer thickness.

Wave-localization theory predicts the spectrum of the one-way transmitted wave. The spectrum of the reflected primary depends on the original source spectrum $S(f)$, the scattering Lyapunov coefficient γ_{exp} , twice the thickness L of the basalt layer, and finally any additional intrinsic attenuation. The latter can be expressed by introducing an intrinsic Lyapunov co-

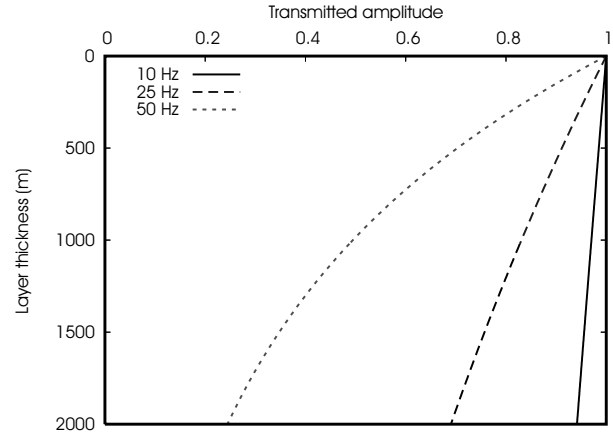


Figure 3 Amplitude of a plane wave traversing the chaotic layer in Fig. 1 for, respectively, a 10 Hz, a 25 Hz and a 50 Hz wavelet. Amplitudes decay exponentially with layer thickness. Clearly, the 10 Hz wavelet is hardly affected by the velocity fluctuations, whereas the 50 Hz wavelet is significantly attenuated.

efficient γ_{in} related to the intrinsic quality factor Q_{in} by

$$\gamma_{in} = \pi f / (c_0 Q_{in}). \quad (6)$$

The spectrum $R(f)$ of the reflected primaries thus becomes

$$R(f) = S(f) \exp[-2(\gamma_{exp} + \gamma_{in})L], \quad (7)$$

where the Lyapunov coefficient γ_{exp} due to scattering is given by expression (5), and the Lyapunov coefficient for intrinsic attenuation is given by equation (6). Equation (7) describes both the effect of the stratigraphic filtering due to apparent scattering losses and the result of any intrinsic attenuation present.

PROPOSED WORK-FLOW

How can we use expressions (5)–(7) to predict the strength and spectrum of target reflections and thereby the possible resolution? The analysis is greatly simplified if a well log is available for the overlying strongly heterogeneous layer or for a similar geology from which we can extract the relative fluctuations δc in the P-wave velocity. These are required to compute the standard deviation σ_c and the typical scale length a . It is advisable to remove any background trends and coarse-scale layering before computing the autocorrelation function, in order to reduce statistical biases. Both the standard deviation σ_c and the typical scale length a are derived by fitting an exponential function through the observed autocorrelation function. The variance σ_c^2 is found at zero lag, and the typical scale length occurs by definition at the lag ζ where $\phi_c(a) = \sigma_c^2 \exp[-1]$ (see equation (3)) (White *et al.* 1990).

If no local or even regional well logs are available, then the only option is to collect a range of possible values for the standard deviation σ_c and scale length a from a literature review, and to perform a series of tests to determine upper and lower bounds for the required source strength and principal frequency.

Next, we need to ascertain what basaltic thicknesses are anticipated in the area of interest, and naturally whether we wish to illuminate sub-basalt structures underneath the thickest packages or only underneath areas of moderate thickness. With this aim in mind, we recommend that first the amplitude decay of the transmitted wave is analysed as a function of layer thickness – analogous to Fig. 3 for the well log shown in Fig. 1. The amplitude decay is computed from equations (1) and (5).

Intrinsic attenuation can be included, if required, by modifying equation (1) to $|T| \propto \exp[-(\gamma_{\text{exp}} + \gamma_{\text{in}})L]$, where the intrinsic Lyapunov coefficient γ_{in} is given by equation (6). This naturally requires knowledge of the anticipated intrinsic quality factor Q_{in} , which may be hard to obtain.

Finally, the expected spectrum of the reflected primaries should be computed for a range of magnitudes σ_c , scale lengths a and thicknesses L , so that a good impression is gained on how variations in these parameters affect the anticipated spectrum. Equations (5)–(7) are required for this. It is recommended that the reflected spectrum is computed, first for a white source $S(f) = 1$ and, subsequently, for the true source spectrum $S(f)$.

NUMERICAL EXAMPLE

To illustrate the whole procedure, we consider a 600 m thick, strongly heterogeneous layer with a background P-wave velocity c_0 of 3500 m/s, a typical scale length $a = 1.5$ m, and a standard deviation of the relative P-wave velocity fluctuations of 25%. These values are based on those derived from a well log through a basalt (Fig. 1). No intrinsic attenuation is included (i.e. $Q_{\text{in}}^{-1} = 0$).

We use a Ricker wavelet to model the source spectrum. It is given by $S_{\text{Ricker}}(f) = (f/f_p)^2 \exp[1 - (f/f_p)^2]$, where f_p denotes the peak frequency. It is scaled such that its maximum of one occurs at the peak frequency.

Figure 2 shows the synthetic sections for a 50 Hz and a 10 Hz Ricker wavelet. Hardly any coherent energy is visible underneath the top-basalt reflection for the high-frequency wavelet, whereas the 10 Hz wavelet reveals several sub-basalt structures.

Figure 3 shows the amplitude of a plane wave traversing the chaotic layer (one-way) for a 10 Hz, a 25 Hz and a 50 Hz wavelet. The 10 Hz wavelet is hardly affected by the velocity fluctuations while the 50 Hz wavelet is significantly attenuated with increasing layer thickness.

Figure 4(a, b) demonstrates the increasing amount of stratigraphic filtering for increasing P-wave velocity fluctuations. All other parameters are kept constant. The monotonically decaying curves (left) are for a white source spectrum ($S(f) = 1$), while the distorted bell-shaped curves (right) show the recorded spectra if Ricker wavelets with peak frequencies of 10 Hz and 50 Hz are used. Multiple scattering is greatly reduced if a low principal frequency is employed. However a 50 Hz source frequency is, in this case, still likely to produce a good imaging quality for velocity fluctuations with a 12.5% standard deviation.

Figure 4(c, d) shows the influence of the thickness L on the recorded spectrum. As expected, the apparent attenuation due to scattering increases with increasing thickness. Higher source frequencies are suitable for thinner basalt layers.

Figure 4(e, f) shows the resulting spectra for various typical scale lengths a . Its effect is less clear cut, although in general, we note that the lower frequencies are increasingly attenuated with increasing scale length. Smaller scale lengths thus allow for higher source frequencies.

DISCUSSION

A close inspection of Figs 3 and 4 reveals that the predicted peak amplitude of the 50 Hz Ricker wavelet is roughly half that of the 10 Hz wavelet for the synthetic model in Fig. 1. Why then do we not see any evidence of sub-basalt structures in the associated 50 Hz synthetic section (Fig. 2, left)? There are several reasons for this.

First, plane waves in horizontally layered media are not subject to geometric spreading (Wang and McCowan 1989; van der Baan 2004). The geometric spreading naturally further reduces the amplitudes. It can be included approximately by multiplying the spectrum R by the compensation factor t^{-n} , where t is the zero-offset traveltime and n is a suitably chosen constant. The choice $n = 2$ is commonly used.

Second, equations (4) and (5) assume that the density is constant, while density fluctuations were included in the synthetic gathers to render them more realistic (Figs 1 and 2). The Lyapunov coefficient (5) thus provides a lower bound. Total attenuation due to scattering will generally be higher due to fluctuations in density. It also tends to increase with increas-

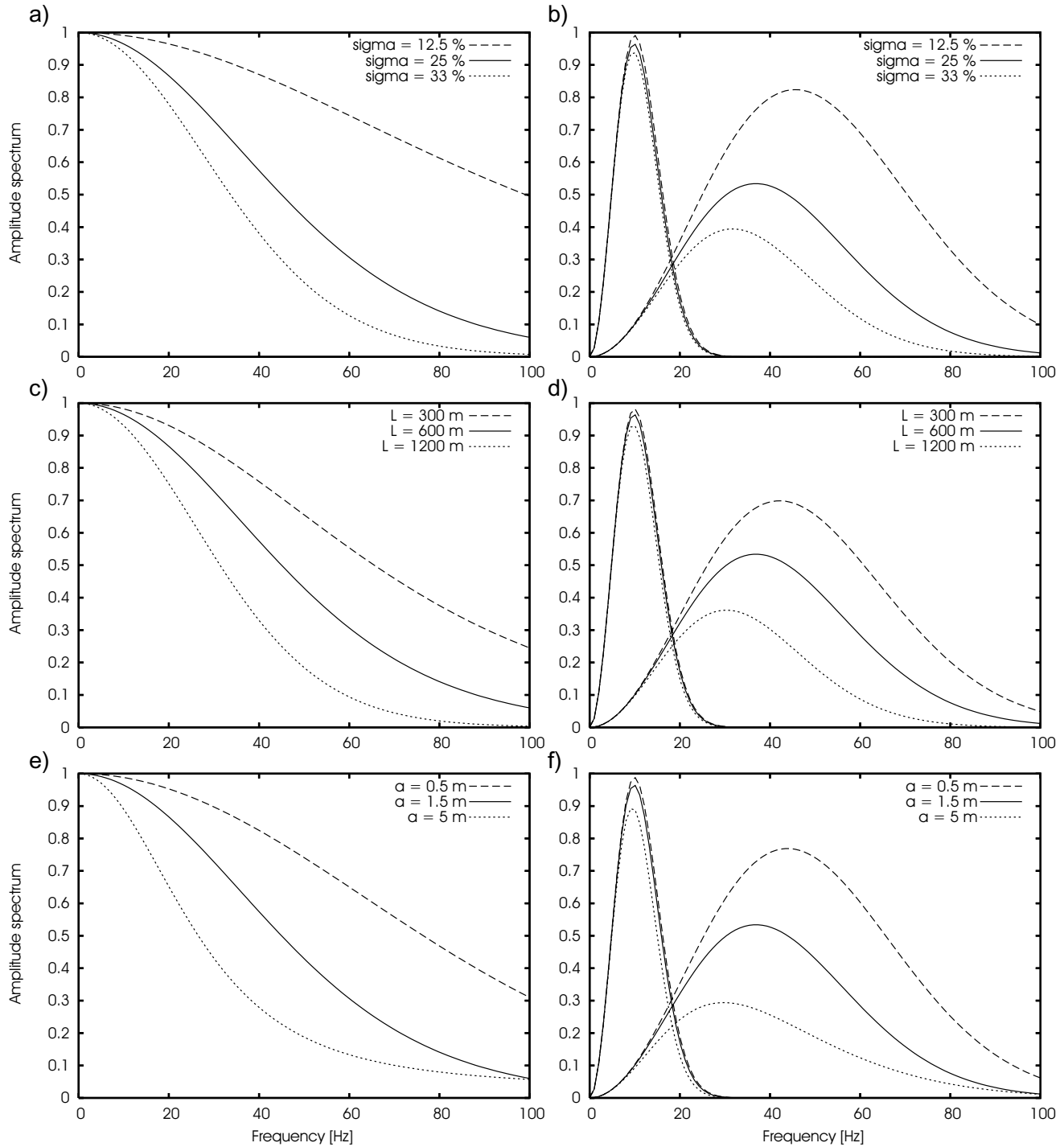


Figure 4 Recorded amplitude spectra for various random media showing the influence of variations in: (a) and (b): the standard deviation σ_c of velocity fluctuations; (c) and (d): layer thickness L ; (e) and (f): scale length a . Continuous line: reference model; dots and dashes: perturbations around reference model. Left: white source spectrum; right: Ricker wavelet with a peak frequency of 10 Hz and 50 Hz, respectively. The 50 Hz wavelet is clearly significantly more attenuated than the 10 Hz wavelet. This explains why only the 10 Hz wavelet distinguishes the sub-basalt reflections, deep 1 and deep 2, in Fig. 2.

ing angle of incidence (Shapiro and Zien 1993; van der Baan 2001).

Third, only acoustic scattering is taken into account in expression (5). This is not a problem at vertical incidence since no P-S conversions occur then. Possible mode conversion also increases the total attenuation of the primary reflections. Shapiro and Hubral (1996) provided appropriate approximations for the Lyapunov coefficient for the elastic case where fluctuations occur in both P- and S-wave velocities and in density.

Finally, wave-localization theory predicts the amplitude of the transmitted wave only. It does not predict the strength of the P-wave coda as a function of time and position (i.e. the pegleg multiples created in the random layer). A complex interplay occurs between the strength of the primaries and their coda, which is influenced by their geometric spreading, the reflection coefficients of the target horizons, and their positions with respect to the bottom of the random layer.

Expressions (5)–(7) are intended to eliminate the need for repeated numerical simulations using a variety of synthetic models to determine the optimum principal source frequency. However, at least one numerical simulation must be performed in order to study the influence of the coda, especially if the target horizon is close to the bottom of the strongly heterogeneous medium.

As a general rule of thumb, an upper limit for the total energy of the P-wave coda is given by $1 - |T|^2$, where T is the transmission coefficient of the transmitted plane-wave pulse (equation (1)). In other words, if the plane-wave pulse is at 50% of its original amplitude, then the total coda-wave energy already represents 75% of the total energy. More comprehensive information on the influence of the P-wave coda can be obtained by combining wave-localization theory with the phenomenological theory of Frankel and Wennerberg (1987) for the coda strength.

A final comment remains to be made concerning the type of autocorrelation function used. It was assumed explicitly in the derivation of the Lyapunov coefficient (5) that the random medium is described by an exponential autocorrelation function. The type of autocorrelation function used is actually related to the rugosity of the medium. An exponential autocorrelation function indicates that the medium is piecewise continuous (van der Baan 2001). Other autocorrelation functions exist. The Von Kármán function, for instance, is very versatile and includes both fractal media and media smoother than those described by an exponential autocorrelation function. Van der Baan (2001, 2002) provided more background and appropriate Lyapunov coefficients.

CONCLUSIONS

Quantitative estimation of source penetration depth is required if source frequencies are lowered to render target horizons underneath basaltic or coal sequences more visible while simultaneously maintaining a suitable resolution. Wave-localization theory is a useful tool to study stratigraphic filtering in chaotic layered lithologies. It predicts the apparent attenuation due to scattering of a plane wave traversing a layer with high velocity fluctuations. It can therefore be used to predict the optimum principle source frequency in the trade-off between loss of resolution and increased penetration depth. This can be done with the help of a few statistical parameters derived from a well-log analysis; namely, the average background velocity, the expected standard deviation in the velocity fluctuations, the typical scale length of the heterogeneities and the thickness of the basalt layer. In the likely event that no local well logs exist, a multitude of scenarios can easily be examined at low cost.

ACKNOWLEDGEMENT

M.v.d B. and J.W. thank Shell EP Europe for financial support.

REFERENCES

- Anderson P.W. 1958. Absence of diffusion in certain random lattices. *Physics Review* **109**, 1492–1505.
- van der Baan M. 2001. Acoustic wave propagation in one-dimensional random media: The wave localisation theory. *Geophysical Journal International* **145**, 631–646.
- van der Baan M. 2002. Constant Q and a fractal, stratified Earth. *Pure and Applied Geophysics* **159**, 1707–1718.
- van der Baan M. 2004. Processing of anisotropic data in the τ - p domain: I – Geometric spreading and moveout corrections. *Geophysics* **69**, 719–730.
- Frankel A. and Wennerberg L. 1987. Energy-flux model of seismic coda: Separation of scattering and intrinsic attenuation. *Bulletin of the Seismological Society of America* **77**, 1223–1251.
- Shapiro S. and Hubral P. 1996. Elastic waves in finely layered sediments: The equivalent medium and generalized O'Doherty and Anstey formulas. *Geophysics* **61**, 1282–1300.
- Shapiro S. and Zien H. 1993. The O'Doherty and Anstey formula and the localization of seismic waves. *Geophysics* **58**, 736–740.
- Wang D.Y. and McCowan D. W. 1989. Spherical divergence correction for seismic reflection data using slant stacks. *Geophysics* **54**, 563–569.
- White B., Sheng P. and Nair B. 1990. Localization and backscattering spectrum of seismic waves in stratified lithologies. *Geophysics* **55**, 1158–1165.
- Ziolkowski A., Hanssen P., Gatliff R., Jakubowicz H., Dobson A., Hampson G., Li X.-Y. and Liu E. 2003. Use of low frequencies for sub-basalt imaging. *Geophysical Prospecting* **51**, 169–182.